Study of translational, librational and intra-molecular motion of adsorbed liquid water monolayers at various TiO_2 interfaces

Ritwik S. Kavathekar[1], Niall J. English[1,2,a)] and J.M.D. MacElroy[1,2]

[1]The SFI Strategic Research Cluster in Solar Energy Conversion, School of Chemical and Bioprocess Engineering and [2]Centre for Synthesis and Chemical Biology University College Dublin, Belfield, Dublin 4, Ireland.

Keywords: Molecular Dynamics, Titania, Water, Vibrational Motion

Equilibrium classical molecular dynamics (MD) simulations have been performed to investigate the vibrational motion of water in contact with rutile-(110), rutile-(100), rutile-(001), anatase-(101) and anatase-(001) surfaces at room temperature (300 K). The vibrational density of states (VDOS) of the first adsorbed monolayer of liquid water has been analysed for each surface. These have been compared with reported experimental INS values involving rutile and anatase polymorph surfaces, along with *ab initio* MD results. It is observed that good qualitative agreement is obtained for the rutile-(110) and the anatase-(101) surfaces with the corresponding experimental VDOS. A significant contribution from librational dynamics is found for planar rutile surfaces, but no such demarcation is seen in the experimental VDOS.

[a)] Corresponding author. Tel: +35317161646. Email: niall.english@ucd.ie

Introduction

In recent years, the study of aqueous solutions in contact with TiO_2 interfaces has become a subject of considerable scrutiny, due in part to its ubiquity in systems for renewable energy applications in photo-electrochemical water splitting or dye-sensitised solar cells, in addition to addressing open questions relating to the super-hydrophilic or super-photo-hydrophobic nature of solvated solutes adsorbed at such surfaces. Such interfaces provide a rich environment for investigation of confinement of water molecules' motion, manifesting varying transport and vibrational properties as a result. This is particularly true where hydrogen-bonded molecules play an important role in stabilising solutes via solvent interactions and forming "cages". Although TiO_2 is one of the most studied metal oxides in the literature, there is somewhat limited understanding of interfacial water molecules' behaviour on TiO_2, despite recent progress in this area.[1]

The dynamical behaviour of interfacial water molecules at titania surfaces has been probed recently by various spectroscopic methods.[2-6] Quasi-elastic neutron scattering (QENS)[4] experiments have shown that hydrogen bonding between the first and second layers of water molecules above rutile-(110) surface stabilise the first monolayer at the interface, providing a less mobile and more ice-like structure quite distinct from that of liquid water. Neutron back-scattering experiments, along with molecular dynamics (MD)[7] studies have shown that detailed hydrogen bonding properties depend on the level of hydration and its dynamical correlation with diffusion and stability. Experimental vibrational density of states (VDOS) spectra of adsorbed water for both rutile rods and anatase powder have been reported[2,3] via inelastic neutron

scattering (INS) measurements, concluding that the confined adsorbed water molecules exhibited vibrational and dynamical features closer to less mobile ice vis-à-vis the liquid. From MD studies, the velocity auto-correlation function (VACF) for water molecules can be extracted as

$$C_{vv}(t) = \frac{1}{N}\sum_{i=1}^{N}\left\langle v_i(t) \bullet v_i(0)\right\rangle \tag{1}$$

whose Fourier transforms gives the VDOS (or power spectrum).[7] The translational DOS of water molecules is characterised primarily by motion of oxygen atoms, while the librational modes arise essentially from proton motion. Such VDOS spectra computed from MD have been useful in characterising the dynamical and vibrational behavior of water molecules with various potential models in the bulk liquid state,[7] adsorbed on metals,[8] rutile-(110) and anatase-(101) surfaces,[9,10] and in contact with biomolecules[11] and in methane hydrates.[12] In particular, *ab initio* MD has offered key insights into the librational motion of higher-frequency modes of water adsorbed to titania in very interesting recent studies,[10,11] but the somewhat restrictive computational limits on *ab initio* MD (AIMD) simulation duration makes it difficult to ascertain lower-frequency translational modes (primarily of oxygen atoms) with a desired level of accuracy.

In this study, we investigate the features of VDOS via equilibrium classical MD simulation, so as to allow for longer-scale sampling vis-à-vis *ab initio* MD, and, therefore, the study of the full frequency range of water VDOS for the monolayer in immediate contact with a variety of rutile and anatase surfaces. In addition, we study the vibrational coupling of the surface layers of water molecules and titania with each other. This allows for at least a qualitative investigation into the molecular mechanisms governing vibrational water behaviour at titania-water interfaces.

Simulation Methodology

As described in our previous MD study of titania-water interfaces,[14] all surfaces were cut from bulk rutile with lattice vectors $a_0 = b_0 = 4.593$ Å, $c_0 = 2.959$ Å (symmetry group *P42/MNM*) and bulk anatase with lattice vectors $a_0 = b_0 = 3.776$ Å and $c_0 = 9.486$ Å (symmetry group *I41/AMD*). The stability of the surfaces are in the decreasing order 110 > 100 > 101 > 001 for rutile and 101 > 001 for anatase. Rutile-(110) and anatase-(101) are the most stable and studied surfaces, for which considerable experimental data are available. The rutile-(110) surface was cut for charge compensation to yield a non-polar and dipole free surface.[1,14] Every titania surface atom has some extent of under-saturation in its coordination. Although rutile-(110) surface atoms have been assigned charges[13] for classical dynamics, we have not applied these in our MD in our simulations so as to enable comparison between different surfaces, and for consistency with our earlier simulation study.[14] Also, specific charges or force-field parameters for atoms on other surfaces are unavailable in the literature. Our previous simulation study of water structural properties also show that charges for bulk rutile work reasonably well for all of the surfaces studied.[14] Rutile-(101) has a natural slanting angle with respect to [001] or the *z*-direction (the direction of heterogeneity, *i.e.*, orthogonal to the surfaces in the *x*-*y* plane) which was corrected by aligning the entire slab orthogonal to the z axis so as to facilitate an orthorhombic periodic box. The surface of rutile-(001) is more acidic due to highly unsaturated four-coordinated Ti atoms. Anatase is the most photoactive polymorph of TiO_2 and is more stable at nanoscale dimension than rutile,[15] and hence is an important surface for study. The anatase-(101) surface is also tilted at an angle and was aligned vis-à-vis the *z*-axis. Although rutile-(001) and anatase-(001) are unstable, and hence the reason for which no comparable neutron scattering data is

available, they have been included in this study for the sake of completeness. The details of the system sizes and simulation box dimensions are specified in Table I.

[insert Table I about here]

The Matsui-Akaogi force-field was applied to titania, and a flexible SPC-type model to water (SPC-Fw).[17] The Ti-water oxygen (Ow) parameter was set to that of the titania Ti-O Buckingham potential and the Ow-oxide oxygen parameters were set to those of the SPC-Fw Lennard-Jones potential. These values are summarised in Table II. The oxide surface was allowed to be fully kept mobile. The Ewald method[7] was used to handle long-range electrostatics to within a relative precision of 10^{-5}, as implemented in the DL_POLY v2 package.[16] MD was performed in a Nosé-Hoover NVT ensemble[7] at 300 K using velocity-Verlet integration with a 0.33 fs timestep, so as to sample adequately high-frequency vibrations of water hydrogen (Hw) atoms. For bulk liquid water, molecules were equilibrated for about 200 ps via the Anderson-Hoover NPT ensemble[7] before performing a 100 ps NVT run at 300 K. Given the less mobile, more solid-like nature of the first water monolayer[10,11,14] (dubbed '1 ML'), an ice-Ih system was equilibrated in the same manner at a temperature of 220 K to avoid melting, using 2x2x2 replication of the orthorhombic 5x3x3-unit cell proton-disordered configuration of Hayward and Reimers (in their *x*, *y*, *z*-laboratory-axis definition).[19] For the titania-water systems, water molecules were added in the *z*-direction, and the whole system was equilibrated for up to 200 ps. Following this, production runs were carried out for 100 ps and snapshots sampled every 1 fs.

[insert Table II about here]

The VACF was calculated for oxygen and hydrogen atoms in the first adsorbed water monolayer, in addition for bulk ice and liquid water, along with their Fourier transforms (power spectra) in the laboratory *x*-, *y*- and *z*-directions, to give direction-resolved (and total) translational and librational DOS, respectively. The (total) VDOS of each system may be compared to recently available INS findings.[2] In addition, the self-diffusion coefficient of these water molecules was calculated via integration of the translational VACF, averaged per molecule[17]

$$D = \frac{1}{3}\int_0^\infty dt \langle v_i(t) \bullet v_i(0) \rangle \qquad (2)$$

taking care to sample the translational VACF (cf. eqn. 1) to sufficient length to allow for its decay to zero, and, hence, for the convergence of the diffusivity estimate of eqn. 2. To assess the extent of isotropy, or otherwise, of the self-diffusivity vis-à-vis the laboratory coordinate system, self-diffusivites were estimated along each of these directions from the corresponding direction-resolved VACF (without the '3' factor in eqn. 2).

Results and Discussion

Prior to discussing the vibrational spectra of the adsorbed water monolayer, and on differences and similarities with respect to ice, liquid water and available INS and AIMD findings, it is instructive to consider briefly monolayer dipolar orientations at the titania surfaces, which were considered in somewhat more detail in our previous studies of water structural properties.[14] Fig. 1 specifies the distributions of cosine of the angle made by the monomer dipole vector with respect to the (laboratory *x*-*y*) plane of the crystal surface. A cosine of zero indicates dipole

alignment normal to the face, while ±1 indicates parallel dipole alignment, *i.e.*, oriented in a parallel manner along the surface. It can be seen clearly that there is a preferential dipole alignment approximately normal to the surface for rutile-110, and oriented at 20-30° from the normal in the case of rutile-101, while rutile-100 and rutile-001 exhibit dipole-alignment along the plane of the surface (in both directions for rutile-001). There is essentially no preferential dipole alignment for anatase-001, while anatase-101 has a preference for 20-30° orientation from the normal. These alignments are as a consequence of physical adsorption in energetically preferred motifs due to the local structure of corrugation, bridging oxygens, transient hydrogen bonds between water-protons and titania (bridging) oxygen atoms, etc. A general trend is that the more perpendicular the orientation, the further away the protons from the surface, thus rendering greater photo-stability, in agreement with observed rankings of photo-reactivity of the surfaces.

[insert Figure 1 about here]

Each surface shall now be considered in detail, in order to study common characteristics of the vibrational spectra of the adsorbed monolayer, and also of liquid water and ice Ih, compared to INS data.[2,3] Crucially, the oxygen- and hydrogen-atom power spectra are discussed in the same context unless otherwise noted so as to enable comparison with AIMD-derived VDOS, which is not decomposed into constituent atoms although the key features of the librational modes are indeed identified for rutile-(110) and anatase-(101) surfaces.[10,11]

Liquid Water and Ice Ih

Classical molecular dynamics simulations were carried out according to the procedure outlined above on an approximately 20 $Å^3$ dimension water box, containing 268 molecules. The VDOS obtained via the Fourier transforms of the VACF for oxygen and hydrogen atoms are presented

in Fig. 2. The VDOS spectra can be divided according to regions of translational and librational components, the range for translational being less than 400 cm^{-1} for oxygen and around 400 to about 1000 cm^{-1} for hydrogen, respectively. Characteristic features of the oxygen spectra include peaks at 45 cm^{-1}, 165 cm^{-1} (shoulder) and 230 cm^{-1} (plateau). The 45 and 230 cm^{-1} peaks are seen in Raman spectra[2,3] and the 165 cm^{-1} peak gives the Einstein frequency of liquid. Water bending (as seen from the hydrogen spectrum) contributes a sharp peak at 1450 cm^{-1}, while the O-H stretch is represented as two sharp peaks at 3556 and 3662 cm^{-1}, rather than a broad spectrum as in AIMD-based VDOS.[9] This broad nature might arise from a lack of a more accurate description of hydrogen bonding in CMD as compared to AIMD, where weak interactions are much more clearly represented giving rise to an energy spread of OH (bs) corresponding to symmetric and anti-symmetric stretch. However, the most likely explanation for the difference in CMD results here with AIMD for intra-molecular frequency modes is that the classical SPC-Fw model has been parameterised to a specific HOH bond angle-frequency and OH stretch frequency, in terms of the force-field coefficients (cf. Table II), while such an approximation is not made in AIMD. As mentioned previously, the total VDOS has been decomposed into its laboratory-frame *x*, *y* and *z* components. Since the bulk liquid environment is isotropic, all contributing components are similar. The self-diffusion coefficient calculated from eqn. 2 (integration of the translational VACF) was found to be 2.25 x 10^{-9} m^2s^{-1}, in excellent accord with the experimental value of 2.3 x 10^{-9} m^2s^{-1},[8] and the previously calculated value for this potential model.[17] All self-diffusion coefficient values are summarised in Table I along with their *x*, *y* and *z* components.

[insert Figure 2 about here]

Since the INS spectra were measured at low temperatures[2,3] (10 and 4 K), the VDOS of ice Ih is used as an additional reference for comparison of the (less mobile) adsorbed water layer at titania surfaces, to present a qualitative picture of monolayer-water spectra. The corresponding oxygen transverse-acoustic band (cf. Fig. 2a) is now shifted upwards by 25 cm^{-1} to 70 cm^{-1}, consistent with a liquid-to-solid phase change, more strongly hydrogen bonded network and lower diffusion values (cf. Table II). This peak is also well-represented in the experimental value of approximately 7 meV (56 cm^{-1}) corresponding to the ice-Ih transverse-acoustic peak, shifted to 70 cm^{-1} due to the simulation being carried out at 220 K to avoid melting. There is also a upward shift in the librational bands from around 400 cm^{-1}, in going to a more hydrogen bonded/constrained state vis-à-vis the liquid. The water-bending band is also up-shifted marginally from 1460 to 1470 cm^{-1}. However, no significant shift is seen in the O-H stretch mode, due primarily to the force-field parameterisation of the O-H stretch mode.

[insert Figure 3 about here]

Rutile-(110) Surface

Rutile-(110) is the most stable surface and hence the most studied. It contains bridging oxygen atoms bonded to 6-coordinated titania (Ti_{6c}) and a 3-coordinated oxygen (O_{3c}) bonded to Ti_{5c} and Ti_{6c} atoms. A dipole-free surface can be constructed by charge compensation by removing the atoms not bonded to these atoms.[1] These Ti_{5c} surface atoms were used as the plane against which height measurements of water oxygen (O_w) atoms were made to isolate the first monolayer of atoms. The VDOS spectra of first monolayer of water oxygen and hydrogen atoms are shown in Figs. 4(a) and 5(a), respectively. The transverse band in the VDOS is now a broad spectrum and has lost its characteristic shoulder and plateau-like nature. A broad band now

appears between 120 and 307 cm^{-1}, with little distinction between peaks. The inter-molecular interactions with its oxygen neighbors in water and ice have now been replaced with Ti and O from the oxide surface. These features match the ones reported in the experiment [2] with a broad spectrum nature at 15 to 40 meV including the absence of the 8 meV peak. Somewhat surprisingly, the *y*-component of the oxygen spectrum is not shifted as much as the *x*- and *z*-components, and is in the range of 62 to 230 cm^{-1}. This corresponds to a less hydrogen-bonded or more 'free' structure, since the water oxygen is buffeted by Ti5c atoms along the *x*-axis and finds a minimum above them as shown in the dipole-angle distribution in Fig. 1(a), while protons are 'pulled' towards the bridging oxygen of the rutile-(110) surface in the *y*-direction. This is also reflected in the hydrogen spectrum where the *y*-component of the VDOS in Fig. 5(a) is shifted to a relatively even distribution in the the 100-500 cm^{-1} range rather than being centered at approximately 550 cm^{-1} in the bulk liquid state. The water-bending mode has shifted from 1470 cm^{-1} in ice Ih to a more strongly distorted 1662 cm^{-1} in the first monolayer at the rutile-(110) interface. Considering the *y*- and *z*-component contributions, it is clear that bending motion takes place in these planes and to a negligible extent in the *z*-plane (*i.e.*, normal to the surface). These bending modes are situated approximately at *circa* 200 meV (about 1620 cm^{-1}) in the experimental spectra,[2,3] and hence give a close match. These peaks are also reported within from AIMD calculation of the rutile-110 surface,[9] and our values are also essentially in agreement.

[insert Figures 4 and 5 about here]

The OH stretch for rutile-(110) is seen as a broad band centered at 3453 cm^{-1}, unlike two distinct peaks for other rutile surfaces. These profiles matches well with experimental INS spectra;[2,3] the experimental peaks are found to be at 412 (3322 cm^{-1}) and 416 meV (3354 cm^{-1}).

This shift could be attributed possibly to the temperature at which the simulations were carried out, *i.e.*, 300 K, as opposed to experimental temperatures in the 4-10 K region, in addition to the already mentioned classical nature of the bond-stretch parameterisation. We calculated self-diffusion coefficients via eqn. 2, and found it to be 0.021 x 10^{-9} m^2s^{-1}, with the highest contribution thereto in the *y*-direction at 0.050 x 10^{-9} m^2s^{-1}. The values reported in the literature for rutile-(110) range from 0.0 to 2.0 x 10^{-9} m^2s^{-1} , using force field methods[18] as a function of slit distance of 0.8 to 2.0 nm, and 0.2 x 10^{-9} m^2s^{-1} in the first monolayer,[19] as studied by AIMD with the PBE functional. The order-of-magnitude difference between our value and AIMD may be explained by a combination of much shorter simulation time and sampling available for AIMD, as well as the inherent difference between the PBE functional and force-field methods.

Rutile-(100) Surface

The rutile-(100) surface is also a stable one and constitutes 20% of the rutile polymorph.[1] The surface is also composed of Ti6c and Ti5c atoms attached to a bridging oxygen (Ob). This Ti5c-Ob-Ti5c plane is inclined at an angle to the z-axis. Together with (110) surface, it forms the non-planar rutile surface. In this surface, the Ob atoms are along the *y*-direction. Due to this inclination, the relaxation direction is now in both in *x* and *y* and more constrained in the *z*-axis, as evidenced clearly from the respective VDOS components in Fig. 4(b). The transverse-acoustic band of the oxygen VDOS is now spread over a longer range of up to 1000 cm^{-1}. The water bending is observed at 1500 cm^{-1}, indicating a more relaxed/weakly bound H-bonded configuration than the rutile-(110) surface. The water monolayer is also more mobile than rutile-(110) and moves in all three directions, although more easily in terms of surface diffusion along the *x*-*y* plane.

Rutile-(101) Surface

The rutile-(101) interface also contributes to a major portion (20%) of bulk rutile.[1] The surface contains Ti5c and O2c atoms. However, these two bonds are differentiated by different bond lengths. The surface when freshly cleaved is tilted to the *z*-axis and has to be rotated for alignment.[1,14] Together with rutile-(001), it constitutes planar surfaces of the rutile polymorph. The oxygen atoms of this surface are along the *y*-axis.[1,14] The DOS for this surface is represented in Fig. 4(c). The transverse-acoustic band is seen to exist as a broad one between around 130 and 315 cm^{-1} with a tail extending to 1000cm^{-1}. Water molecules in the first monolayer are oriented at 20-30° from the normal (cf. Fig. 1a). Again, a similar trend is evident in localisation of the water monolayer, but the *x*-component of the transverse-acoustic band is broader than those of the *y*- and *z*-components, suggesting stabilisation by two Ti5c surface atoms, rather than one. The rutile-(101) surface shows strong librational peaks at 763 and 924 cm^{-1}, as observed in the experimental spectrum.[2] These peaks are present in other non-planar rutile surfaces as broad features or tail-ends, but are more pronounced in the planar surfaces of rutile-(101) and rutile-(001). The water bending peak appears at 1522 cm^{-1} with a slightly more substantial component in the *y*-direction. This is also reflected in the more significant *y*-component of the OH stretch (at 3571 cm^{-1}), suggesting that more free proton vibration in the *y*-direction, while higher-frequency OH stretch is observed at 3663 cm^{-1}, primarily in the *x*- and *z*-directions.

Rutile-(001) Surface

Rutile-(001) contributes a relatively minor component towards bulk rutile,[1] and is unstable, but has been is included in this study for the sake of completeness. This rutile surface is more acidic due to four-coordinated Ti atoms (Ti4c) and hence affects pH and electrochemical scale to a larger extent. These Ti4c atoms alternate with Ti6c atoms connected via O2c linkages. These

cross-links form ridge-like structure, but retain their overall planar nature. The oxygen VDOS is represented in Fig. 4(d), showing no significant change in the transverse-acoustic band, and appearing with a range of around 120 to 320 cm^{-1}, with all components contributing essentially equally. Again, strong librational peaks appear at 716 and 1015 cm^{-1} peak (somewhat broader, primarily in the *z*-direction); this serves to emphasise the importance of out-of-plane librations in the water monolayer at this surface, due to promotion of rotation oscillations normal to the plane by 'flipping' between two oppositely-oriented dipolar oritentations along the surface (cf. Fig. 1 a, *vide infra*). Unlike the rutile-(101) surface, the OH stretch bands contribute evenly and are found at 3538 and 3656 cm^{-1}. The water monolayer has two distinct dipolar orientations, and flipping occurs between these in order to interact with open O2c atoms at the surface.

Anatase-(101) Surface

The anatase-(101) surface is the most stable and most photo-active titania surface.[1] It has important applications in solar energy harvesting and catalysis. The anatase-(101) surface, exhibits a terrace-like structure formed by fully-coordinated Ti6c atoms bonded to O3c atoms and under-coordinated Ti5c with O2c. The surface is tilted at an angle with respect to the [101] direction, and was rotated to align with the z-axis.[14] The VDOS spectrum is shown in Fig. 4(e). The transverse-acoustic band shows a similar profile to those of bulk liquid water or ice Ih with the same shoulder and plateau regions ranging from 90 to 350 cm^{-1} and two peaks centered at 123 and 288 cm^{-1}. The plateau region is contributed to by the *x*- and *z*-components of the water oxygen DOS. Again, the ice transverse-acoustic peak at 7 meV (about 56 cm^{-1}) is missing in both the anatase experimental[3] and simulated spectrum of this study. The water bending mode is seen at 1460 cm^{-1} and the OH stretch at 3600 and 3669 cm^{-1}. A slight hump is seen at 3538 cm^{-1} for the *x*-component of proton VDOS, which may correspond to a softening of the OH stretch band

seen as a broad range in the 350 to 400 meV in the experimental INS spectrum.[3] This discrepancy may arise from the lack of accuracy of force-field methods in describing the hydrogen-bonding environment, but is more likely due to the empirical nature of the O-H stretch in the force-field as parameterize for bulk liquid water.[17]

Anatase-(001) Surface

The anatase-(001) surface is not stable, and various instances of this have been reported.[1] Anatase-(001) has a flat plane connected by alternating rows of Ti_{5c} and O_{2c} atoms in a three- and two-fold manner, respectively;[1,14] it also contributes to the planar anatase surface. The transverse-acoustic bands from in the translational spectrum are observed over a broad range from 55 to about 200 cm^{-1} (cf. Fig. 4(f)) and it does not have the more "water-like" profile as in anatase-(101). This suggests that water is not adsorbed as tightly by the oxide surface, and this is also reflected in the downward-shifted translational DOS signal vis-à-vis anatase-(001). In parallel, the absence of these peaks in the experimental INS spectrum[3] overlap with these observations. The water bending peak is observed at 1479 cm^{-1} whose *z*-component contribution is slightly more substantial. The water OH stretching modes are seen at 3584 and 3674 cm^{-1}. Anatase-(001), being planar, exhibits a higher self-diffusion coefficient in its water monlayer (about half that of liquid water, cf. Table II), and a broader, essentially featureless distribution profile in the dipolar angle made with respect to the surface (cf. Fig. 1(b)).

Conclusions

DOS spectra calculated via Fourier transformation of the oxygen and proton VACF's of the first monolayer of water above various TiO_2 surfaces have indicated the frequency modes of translational, librational and intra-molecular motion, as derived from classical molecular

dynamics. These have been compared with reported experimental INS values involving rutile and anatase polymorph surfaces, along with AIMD results. It ought to be noted that the self-diffusion coefficients, calculated from equation 2, are from sampling over a period of 100 ps, and this represents a very short time to converge to meaningful values; as such they must be treated with some degree of caution. At the various surfaces, the water molecules are straddled thereon, and are unable to move much beyond the immediate local cage during the short course of the simulations. A detailed description of the effect of hydrogen bonding of water hydrogen atoms to the various surface has been discussed[9,10,20] on various TiO_2 faces. Cummings *et. al.* have studied [4] multi-layer water absorption via neutron scattering and molecular dynamics. They report that diffusivity of water increases away from the surface. Such hydrogen bonding, along with strong Ti-Ow interactions, creates a potential well for the water molecules where they show a high residence time[21]. The reported values (cf. Table I) are reflective of the translational motion peaks observed for all the surfaces in both the experimental and simulated VDOS results, for which very little movement of the water molecules are observed vis-à-vis the liquid state. The diffusion coefficients in Table I support the finding of an absence/suppression of translational motion peaks for water oxygen atoms (cf. Fig. 4) at all interfaces for a relatively short sampling period.

It is observed that good qualitative agreement is obtained for the rutile-(110) and the anatase-(101) surfaces with the corresponding experimental VDOS. A significant contribution from librational dynamics is found for planar rutile surfaces, but no such demarcation is seen in the experimental VDOS. Although most of the shifts in frequency modes may be attributed to hydrogen bonding upon differing adsorption motifs (as suggested by differing dipole-orientation distributions, cf. Fig. 1), a clear description of such bonding may well be too approximate in a

forcefield-based method to register essentially quantitative agreement with hydrogen-bond distance and frequency shifts; in addition, the intra-molecular modes have been parameterised for liquid water, and an implicit assumption is that the adsorption is physical in nature (although recent AIMD treatment of rutile-110 supports this view).[21] In any event, given the length- and time-scale limitations of AIMD to obtain reliable statistics for VACF's and to sample timescales necessary for adequate characterization of translational modes (especially transverse-acoustic), the good qualitative agreement of this classical MD approach with INS spectra underlines the utility of such methods for preliminary investigation of water structure and dynamics at titania surfaces.

Acknowledgements

The authors acknowledge useful conversations with Dr. Damian Mooney and Prof. Nancy Ross. This material is based upon works supported by the Science Foundation Ireland (SFI) under Grant No. [07/SRC/B1160], in addition to the Irish Research Council for Science, Engineering and Technology. We thank SFI and the Irish Centre for High-End Computing for the provision of high-performance computing facilities. The authors acknowledge the support of industry partners to the Cluster: SolarPrint, Celtic Catalysts, Glantreo, Mainstream Renewable Power, Kingspan and SSE Renewables.

References

(1) Diebold, U. *Surface Science Reports* **2003**, *48*, 53.

(2) Spencer, E. C.; Levchenko, A. A.; Ross, N. L.; Kolesnikov, A. I.; Boerio-Goates, J.; Woodfield, B. F.; Navrotsky, A.; Li, G. *The Journal of Physical Chemistry A* **2009**, *113*, 2796.

(3) Levchenko, A. A.; Kolesnikov, A. I.; Ross, N. L.; Boerio-Goates, J.; Woodfield, B. F.; Li, G.; Navrotsky, A. *The Journal of Physical Chemistry A* **2007**, *111*, 12584.

(4) Mamontov, E.; Vlcek, L.; Wesolowski, D. J.; Cummings, P. T.; Wang, W.; Anovitz, L. M.; Rosenqvist, J.; Brown, C. M.; Sakai, V. G. *Journal of Physical Chemistry C* **2007**, *111*, 4328.

(5) Mamontov, E.; Wesolowski, D. J.; Vlcek, L.; Cummings, P. T.; Rosenqvist, J.; Wang, W.; Cole, D. R. *Journal of Physical Chemistry C* **2008**, *112*, 12334.

(6) Mamontov, E.; Vlcek, L.; Wesolowski, D. J.; Cummings, P. T.; Rosenqvist, J.; Wang, W.; Cole, D. R.; Anovitz, L. M.; Gasparovic, G. *Physical Review E* **2009**, *79*.

(7) English, N. J.; Macelroy, J. M. D. *Molecular Physics* **2002**, *100*, 3753.

(8) Loong, C. K.; Iton, L. E.; Ozawa, M. *Physica B: Condensed Matter* **1995**, *213-214*, 640.

(9) Kumar, N.; Neogi, S.; Kent, P. R. C.; Bandura, A. V.; Kubicki, J. D.; Wesolowski, D. J.; Cole, D.; Sofo, J. O. *The Journal of Physical Chemistry C* **2009**, *113*, 13732.

(10) Mattioli, G.; Filippone, F.; Caminiti, R.; Bonapasta, A. A. *The Journal of Physical Chemistry C* **2008**, *112*, 13579.

(11) Russo, D.; Teixeira, J.; Kneller, L.; Copley, J. R. D.; Ollivier, J.; Perticaroli, S.; Pellegrini, E.; Gonzalez, M. A. *Journal of the American Chemical Society* **2011**, *133*, 4882.

(12) English, N. J.; Tse, J. S.; Carey, D. J. *Physical Review B* **2009**, *80*, 134306.

(13) Bandura, A. V.; Kubicki, J. D. *Journal of Physical Chemistry B* **2003**, *107*, 11072.

(14) Kavathekar, R. S.; Dev, P.; English, N. J.; MacElroy, J. M. D. *Molecular Physics* **2011**.

(15) Barnard, A. S.; Curtiss, L. A. *Nano Letters* **2005**, *5*, 1261.

(16) W. Smith, M. L., T.R. Forester *The DL_POLY_2 User Manual*, v. 2.14 ed., 2003.

(17) M. P. Allen ; Tildesley, D. J. Computer simulation of liquids; Oxford University Press, USA, 1989.

(18) Wei, M.-J.; Zhou, J.; Lu, X.; Zhu, Y.; Liu, W.; Lu, L.; Zhang, L. *Fluid Phase Equilibria* **2011**, *302*, 316.

(19) Liu, L.-M.; Zhang, C.; Thornton, G.; Michaelides, A. *Physical Review B* **2010**, *82*, 161415.

(20) Sumita, M.; Hu, C.; Tateyama, Y. *The Journal of Physical Chemistry C*, *114*, 18529.

(21) Koparde, V. N.; Cummings, P. T. *Journal of Physical Chemistry C* **2007**, *111*, 6920.

Phase (surface), X, Y, Z (Å)		System Size	Diffusion Coefficient [x 10^{-9} m^2s^{-1}] (x,y,z)
Rutile (110)	26.26, 45.47, 69.490	$(TiO_2)_{630}$ $(H_2O)_{2000}$	0.021 (0.002, 0.050, 0.012)
Rutile (100)	22.97, 26.63, 70.00	$(TiO_2)_{405}(H_2O)_{950}$	0.587 (0.619, 0.712, 0.428)
Rutile (101) 113.47	27.33, 27.56,	$(TiO_2)_{300}(H_2O)_{2468}$	0.180 (0.191, 0.213, 0.134)
Rutile (001) 124.00	22.97, 22.97,	$(TiO_2)_{400}$ $(H_2O)_{1720}$	0.092 (0.125, 0.105, 0.045)
Anatase (101)	71.46, 26.43, 72.680	$(TiO_2)_{1176}$ $(H_2O)_{3162}$	0.716 (0.727, 0.746, 0.676)
Anatase (001)	33.98, 33.98, 124.00	$(TiO_2)_{648}(H_2O)_{3900}$	1.275 (1.08, 1.53, 1.21)
Liquid Water	20.00, 20.00, 20.00	$(H_2O)_{268}$	2.25
Ice Ih	48.27, 50.17, 47.30	$(H_2O)_{2880}$	0.060

Table I: Details of geometries used and laboratory-frame-resolved self-diffusion coefficients (see text).

Buckingham potential for TiO_2 and water oxygen : $A_{ij} \times exp(-r_{ij}/\rho_{ij}) - C_{ij}/r_{ij}^6$			
i – j	A_{ij}(kcal mol^{-1})	ρ_{ij}(Å)	C_{ij}(kcal mol^{-1} Å^6)
Ti – O	391049.1	0.194	290.331
Ti –Ti	717647.4	0.154	121.067
O – O	271716.3	0.234	696.888
Ti –Ow	28593.0	0.265	148.000
Lennard-Jones potential for water: $(q_i q_j/r_{ij}) + \varepsilon_{ij}[(\sigma_{ij}/r_{ij})^{12}-(\sigma_{ij}/r_{ij})^6]$			
i – j	ε_{ij} (kcal mol-1)	σ_{ij}(Å)	
Ow – Ow	0.1554	3.165492	
Harmonic potential for water: $k/2 \times (r_{ij}-r_0^2)$			
i – j	k_{ij} (Å^{-1})	r^0_{ij} (Å)	
O_w – H_w	1059.162	1.012	
Harmonic angle bending potential for water: $k/2 \times (\theta - \theta_0)$			
i – j – k	θ_0 deg	k (kcal mol^{-1}rad^{-2})	
H – O – H	113.24	75.900	
Atomic charges: q(Ti) = 2.196 *e*, q(O) = -1.098 *e*, q(O_w) = -0.82 *e*, q(H_w) = 0.41 *e*; O_w, H_w = water oxygen and hydrogen atoms			

Table II: Force-field parameters

Figure 1

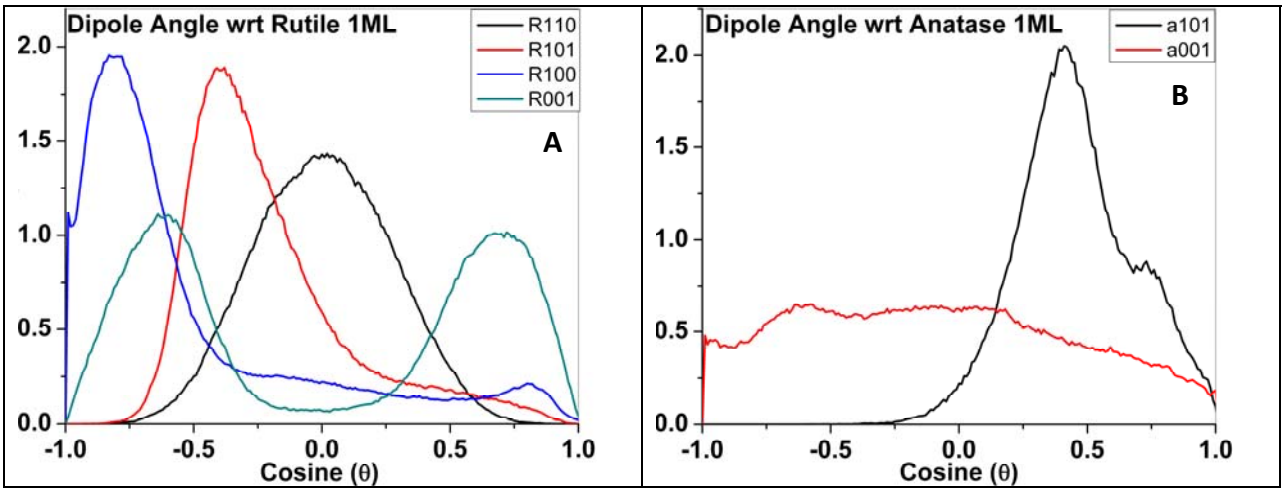
Dipole Angle wrt Rutile 1ML
R110
R101
R100
R001
A
2.0
1.5
1.0
0.5
0.0
-1.0
-0.5
0.0
0.5
1.0
Cosine (θ)
Dipole Angle wrt Anatase 1ML
a101
a001
B
2.0
1.5
1.0
0.5
0.0
-1.0
-0.5
0.0
0.5
1.0
Cosine (θ)

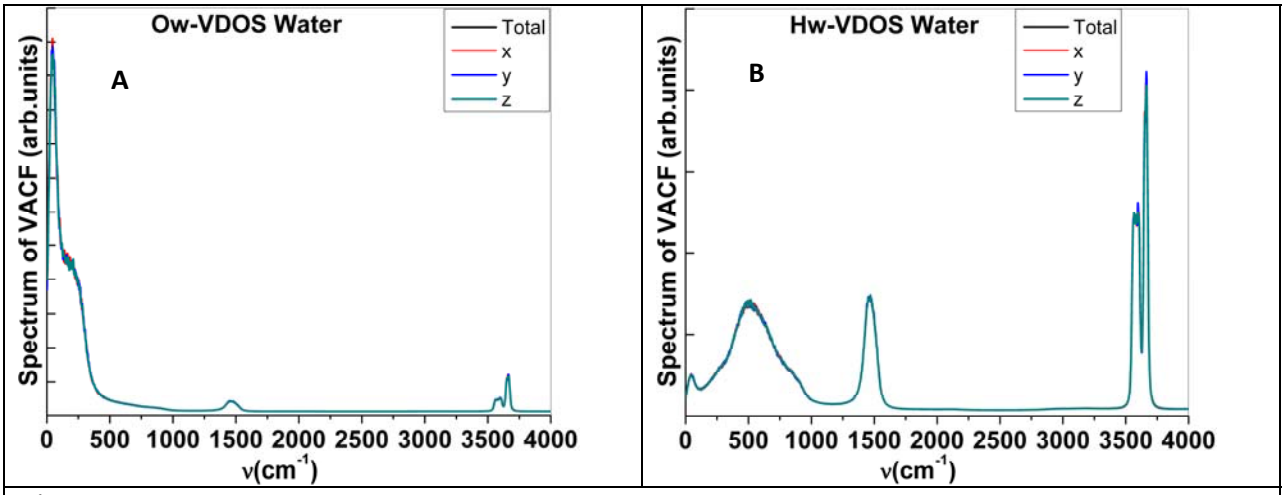

Figure 2

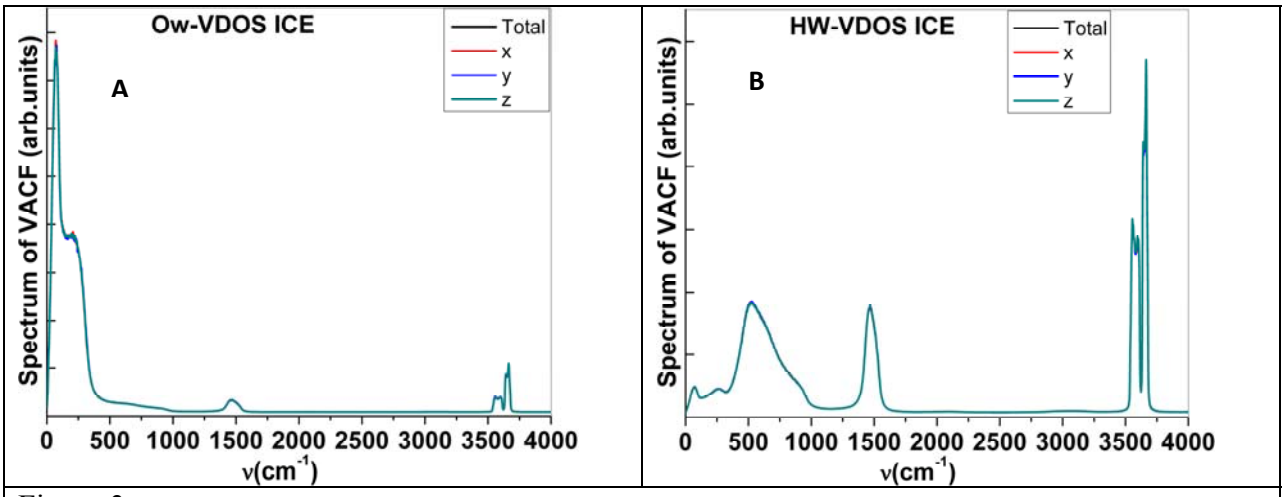

Figure 3

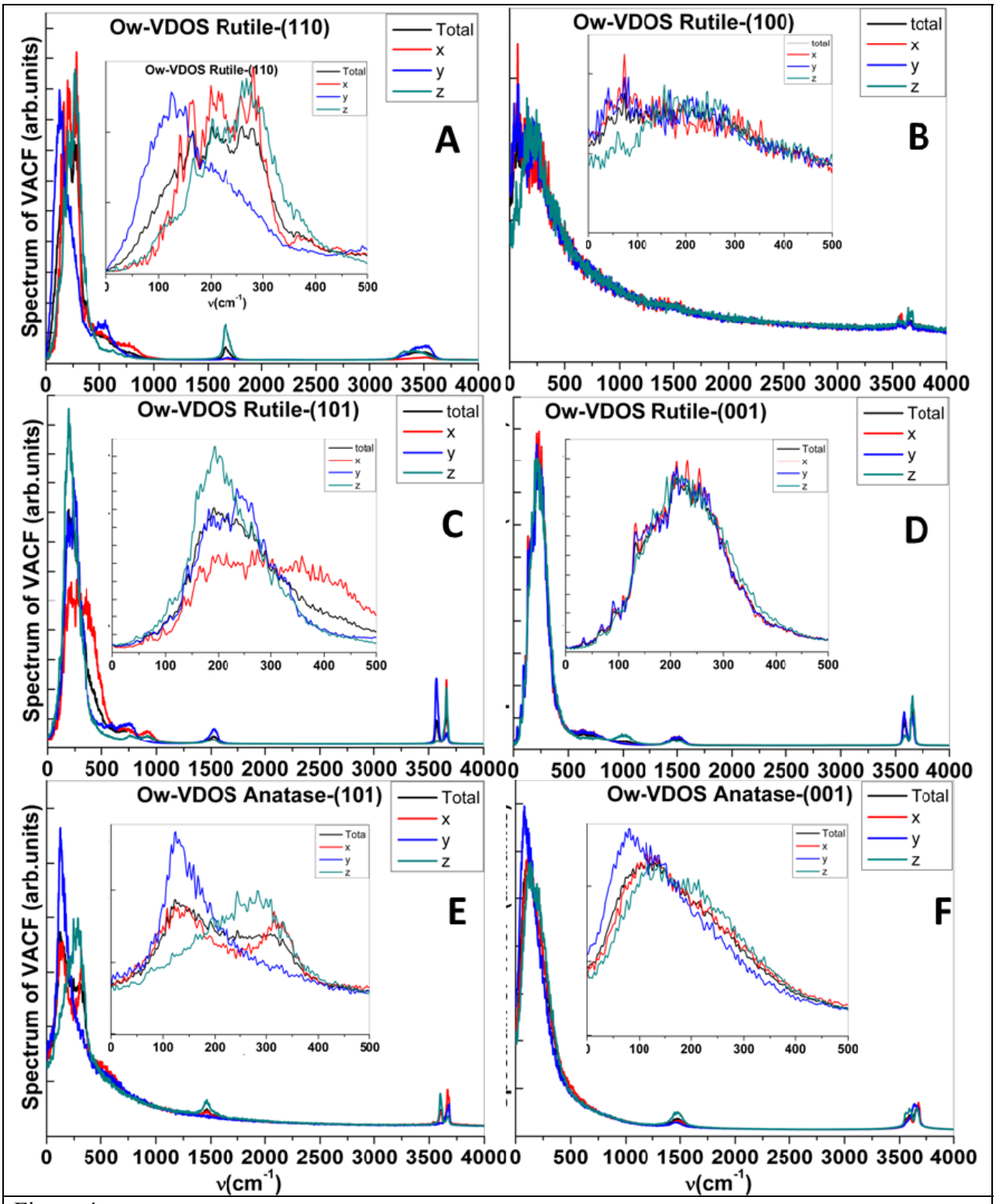
Ow-VDOS Rutile-(110)
Ow-VDOS Rutile-(100)
Ow-VDOS Rutile-(101)
Ow-VDOS Rutile-(001)
Ow-VDOS Anatase-(101)
Ow-VDOS Anatase-(001)
Total
x
y
z
A
B
C
D
E
F
Spectrum of VACF (arb.units)
ν(cm-1)
0 500 1000 1500 2000 2500 3000 3500 4000
0 100 200 300 400 500

Figure 4

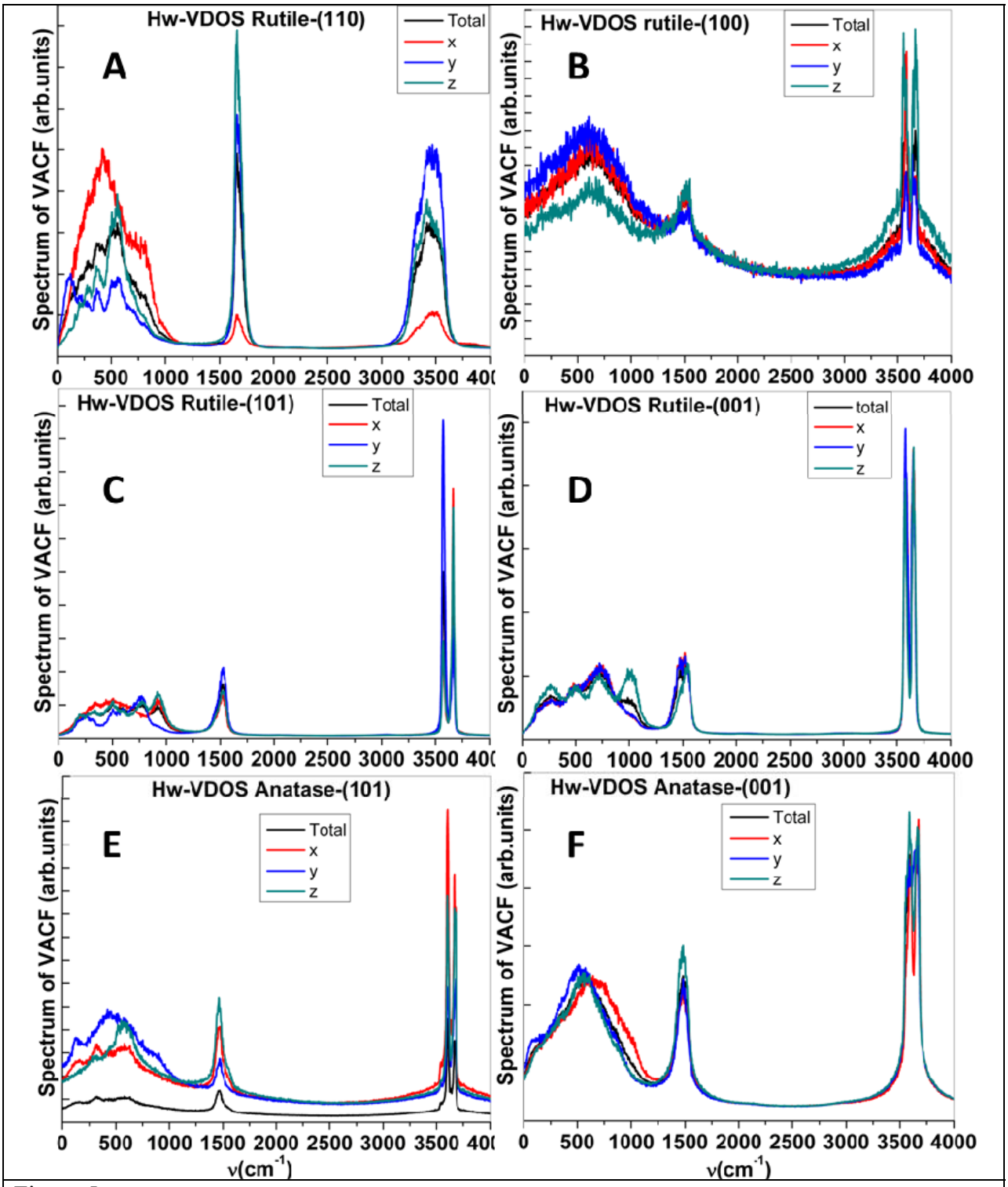
Hw-VDOS Rutile-(110)
A
Total
x
y
z
Spectrum of VACF (arb.units)
Hw-VDOS rutile-(100)
B
Hw-VDOS Rutile-(101)
C
Hw-VDOS Rutile-(001)
D
total
Hw-VDOS Anatase-(101)
E
Hw-VDOS Anatase-(001)
F
Tctal
0 500 1000 1500 2000 2500 3000 3500 4000
ν(cm-1)

Figure 5